ELSEVIER

Food Control 11 (2000) 103–120

FOOD CONTROL

www.elsevier.com/locate/foodcont

On-line system identification and control design of an extrusion cooking process: Part I. System identification

Timothy A. Haley [a,*], Steven J. Mulvaney [b]

[a] Department of Food Science, Purdue University, West Lafayette, IN 47907, USA
[b] Department of Food Science, Cornell University, Ithaca, NY 24853, USA

Abstract

A systems analysis of an extrusion cooking process for puffed corn snack products revealed that the specific mechanical energy (*SME*) and screw speed (*SS*) was a desirable pairing of measured and manipulated variables, respectively for regulating extrudate density. To facilitate the design of an *SME* model-based control system, a discrete-time transfer function that depicts the dynamic response of motor load (*ML*) to changes in *SS* is required. The research literature describes several off-line techniques for developing such transfer function models but no methods for on-line system identification were found. This paper represents the first of two articles that describe our investigations into the use of on-line system identification for automatic tuning and adaptive control of a high-shear twin-screw extrusion process. This paper reports results for using various system identification schemes in combination with relay-feedback as a way to derive, in real-time, a transfer function model that accurately depicts the dynamical behavior of an extrusion cooking process. A Wenger TX-52 co-rotating twin screw extruder was subjected to relay feedback during the processing of cornmeal for a breakfast cereal formula under different moisture and screw speed conditions. The data obtained from these experiments were used to derive first-, second- and third-order discrete-time transfer functions. An analysis of the resulting transfer functions revealed that a first-order lead-lag transfer function structure adequately described the dominant dynamic behavior of the process in all cases. Next, batch and recursive implementations of least-squares, extended least-squares, output error, maximum likelihood, Box–Jenkins and predictive error algorithms were used to derive parameters for the first-order transfer function. Overall, the batch output error method provided good transfer function estimates over the range of product and process conditions studied.

Keywords: System identification; Extrusion cooking; Transfer function; Modeling; Dynamics; Process control; Automatic tuning; Adaptive control

List of symbols

SS	screw speed (rpm)
SS_r	rated screw speed (rpm)
FR	feed rate of ingredients other than water added (kg/min)
P_r	rated motor power (kJ/s)
ML	motor load (%)
MC	melt moisture content (% wet basis)
TM	temperature of the melt at the die (°C)
WA	water added (kg/min)
FM	feed moisture (% wet basis)
DP	die pressure (kPa)
SME	specific mechanical energy (kJ/kg)
e	stationary, white, normally distributed random disturbance variable
k	discrete time sampling instant
a_n, b_n, c_n, d_n, f_n	parameters of the z-transform models in polynomial form. The parameters represent the coefficients of the polynomials A, B, C, D and F, respectively. The index of each coefficient is designated by a value n
$\alpha_n, \beta_n, \gamma_n, \delta_n, \phi_n$	parameters of the z-transform models in pole–zero form. The parameters represent the roots of the polynomials A, B, C, D and F, respectively. The index of each root is designated by value n
K	gain for zero–pole transfer function models

* Corresponding author. Tel.: +1-765-494-9093.
E-mail addresses: haleyt@foodsci.purdue.edu (T.A. Haley), sjm7@cornell.edu (S.J. Mulvaney).

0956-7135/00/$ - see front matter
PII: S0956-7135(99)00068-7

RMS	root mean squared error
PRBS	pseudo random binary sequence

1. Introduction

1.1. Extrusion processing

Over the past several decades, twin-screw extrusion cooking has become a popular method to manufacture ready-to-eat cereal products such as breakfast cereals and snack foods. In large part, this popularity is due to the extraordinary capability of the twin-screw extruder to combine blending, bioreaction, cooking, puffing and forming operations into one efficient continuous process. In particular, extrusion cooking provides a unique means of producing puffed products by the flash evaporation of water upon passing through the extruder die. However, the development of a 'turn-key' automatic extruder control system has been hampered by the general lack of insight into the complex transport properties that occur during extrusion processing and their relationship to finished product quality. Consequently, investigators working in this area have developed mathematical models that attempt to describe the extrusion cooking process to aid in automatic process control design. Models based on first principles have been developed by several investigators for twin screw extrusion cooking processes (e.g., Kulshreshtha, Zaror & Jukes, 1991a; Kulshreshtha Zaror, Jukes & Pyle, 1991b; Tayeb, Vergnes & Valle, 1989; Kulshreshtha, Zaror & Jukes, 1995; Mohamed & Ofoli, 1990; van Zuilichm, van der Laan & Kuiper, 1990), but it is difficult to use such mechanistic models as the basis for an automatic control system. Such models require extensive knowledge of engineering properties that describe the chemical, rheological and physical, and thermodynamic properties of the plasticized biopolymer melt and their interactions within the extruder. Many of these properties and their transport processes in general are either unknown or not well defined for the extreme process conditions that exist within an extruder during operation. In addition, first principles models do not depict the stochastic disturbances characteristic of extrusion processing. The appearance of non-homogeneous feedstock components, transient surging behavior, low frequency vibration harmonics from the rotating screws and sensor noise can contribute to stochastic disturbances that vary depending on the feedstock composition, screw configuration and operating conditions used. Such disturbances are important in the context of control design.

While first principle models can be useful for extruder equipment design, experimentally determined transfer function models are generally used for controller design. Furthermore, any stationary non-white stochastic disturbance present in the process can be suitably modeled by filtering white noise through a transfer function. Transfer function models are developed from observations of the input–output behavior of a process. Typically, the identification of a transfer function is made by first conducting an experiment where the process is subjected to a change in some manipulated variable and measuring the response of one or more output variables. A parameter estimation algorithm is then used to find a transfer function that best describes the observed input–output response.

Transfer functions for extrusion cooking processes have been derived using continuous-time transfer functions (Moreira, Srivastava & Gerrish, 1990; Lu, Mulvaney, Hsieh & Huff, 1993; Cayot, Bounie & Baussart, 1995), as well as discrete-time transfer functions (Hofer & Tan, 1993; Chang & Tan, 1993a; Chang & Tan, 1993b). In those studies, all system identification was performed using *off-line* experiments followed by off-line development of transfer function models. In many cases, it was reported that the transfer functions were subsequently used to derive automatic controllers. However, the controllers developed were only suitable for the limited process and operating conditions studied during the system identification experiments. Given the wide range of dynamic behavior that can result from varying product and processing conditions, many investigators have concluded that some means of *on-line* system identification for automatic tuning and adaptive control of extrusion processing is desirable (Moreira et al., 1990; Kulshreshtha et al., 1991a; Hofer & Tan, 1993; Kulshreshtha et al., 1995). However, a feasible method for on-line identification of the dynamic behavior of extrusion cooking processes has not been reported to date. This paper represents the first of two articles that describe our investigations into the development of an on-line system identification procedure for use in automatic tuning and/or adaptive control of high-shear twin-screw extrusion processes. The contribution reported in this paper is the comparative evaluation of several on-line system identification methods for use with a twin-screw extrusion cooking process. The second paper will focus on the use of such a system for automatic control of puffed corn snack density.

1.2. Systems analysis of extrusion cooking

Although many different cereal products are made using extrusion cookers, each process shares some common process characteristics relevant to process control (Fig. 1). In a typical extrusion cooking process, the manipulated variables are dry ingredient feed rate (*FR*), added water (*WA*), screw speed (*SS*) and barrel jacket temperature (*BT*). The process variables are in-barrel melt moisture content (*MC*) calculated from *WA*

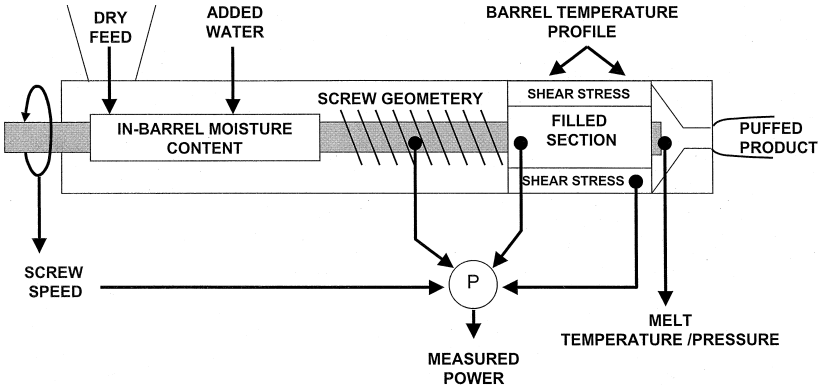

Fig. 1. Process variables available for measurement and control in twin screw extrusion cooking processes.

and feed moisture (*FM*), percent motor power consumed as indicated by motor load (*ML*), pressure at the die (*DP*), and product melt temperature (*TM*). Thus, from a systems perspective, extrusion cooking can be viewed as a 4 input × 4 output process. To facilitate system identification for subsequent control design, it is desirable to reduce, if possible, the dimensionality of the system to be controlled. This can often be done by applying a systems analysis whereby those process variables that have little or no correlation to the product quality characteristics of interest are eliminated from the pool of available inputs and outputs.

1.3. Selection of controlled variables

Numerous experimental studies have demonstrated the importance of specific mechanical energy (*SME*) in high shear extrusion cooking processes. *SME* was first identified as a system parameter, along with specific thermal energy input and residence time distribution, by Meuser, van Lengerich and Kohler (1982). *SME* is referred to as a system variable because it is affected by virtually all extrusion formula and process parameters, and in turn affects the melt temperature and degree of polymerization of starch (van Lengerich, 1990). The vast majority of cereal and/or snack food extrusion cooking processes are conducted at in-barrel moisture contents of about 30% or less. Under these conditions, most (or all) of the energy input into the process is reflected by the SME, due to very limited (if any) heat transfer into the melt via barrel heating. Therefore, a systems analysis view of a reproducible extrusion cooking process might be stated as the application of the same shear stress, as indicated by *SME*, to a melt of the same rheology, which is largely determined by its in-barrel moisture content. All other things being equal, this combination should also provide a reproducible melt temperature and extrusion pressure at the die. Alternatively, manipulation of SME would be a powerful and convenient means of altering the thermomechanical treatment during an extrusion cooking process and manipulating extrudate characteristics. Thus, it remains to select a manipulated variable to pair with *SME* in a closed loop controller.

SME has been recently identified by several researchers in the field as a critical variable for process control in some high-shear twin screw extrusion processes (Lu, Hsieh, Mulvaney, Tan & Huff, 1992; Lu et al., 1993; Onwulata, Mulvaney & Hsieh, 1994). In fact, experimental studies have demonstrated that at steady state, *SME* is highly correlated with *TM* and that extrudate density is highly correlated with *SME* and *MC* (Onwulata et al., 1994). This suggests that *SME* could be used in lieu of *TM* as a controlled process variable for regulating extrudate density in high-shear (low moisture) extrusion cooking processes.

1.4. Selection of a manipulated variable

Within a manufacturing setting, controller design must consider production objectives as well as quality objectives. Process efficiency is maximized when *FR* is set for a high throughput. This constraint practically eliminates *FR* as a manipulated variable. For high shear, low moisture extrusion cooking, *BT* has a negligible influence on *SME* as discussed above. Consequently, of all the manipulated process variables available, *SS* appears best suited for controlling *SME*. This observation was also reported by Onwulata et al. (1994). It should be pointed out that moisture content has a large effect on *SME* at moisture contents less than about 30%. However, the view taken here is that the moisture content in a sense determines the 'polymer' being extruded, and should be controlled to a particular level by the amount of water added to the dry feed. In this way, control of *SME* can then be considered as a means of controlling the exit temperature and/or molecular degradation properties of this base polymer. A second manuscript will demonstrate how *SME* can be used as an indirect means of regulating extrudate density in a high shear

extrusion puffing process. However, given that the extrusion dynamics are strongly affected by moisture content, which is also a primary formulation specification, it would be desirable to determine the dynamics on-line so that an *SME* regulator could be tuned based on current dynamic behavior.

1.5. Variable reduction

Using the foregoing analysis, the system dimensionality can be reduced from 4 inputs × 4 outputs to 1 input (*SS*) × 1 output (*SME*). However, *SME* is not truly a measured variable but rather a function, as shown in Eq. (1), of several process variables *SS*, *ML*, *FR* and *WA*. Since *ML* is the only output variable in Eq. (1), it is clear that the dynamic response of *SME* to changes in *SS* originates from the dynamic response of *ML* to changes in *SS*.

$$SME(\mathrm{kJ/kg}) = P_r(\mathrm{kJ/s}) \cdot 60(\mathrm{sec/min}) \cdot \frac{SS(\mathrm{rpm})}{SS_r(\mathrm{rpm})} \cdot \frac{ML(\%)}{FR(\mathrm{kg/min}) + WA(\mathrm{kg/min})}. \quad (1)$$

Therefore, a transfer function that models the dynamic response of *ML* to changes in *SS* is required. Once such a transfer function is available, it is then relatively straightforward to use Eq. (1) to model the complete response of *SME* to changes in *SS*.

1.6. System identification

A typical system identification procedure is to first conduct an experiment whereby one or more manipulated variables are modulated to excite the process dynamics. Second, a parameter estimation algorithm is used to find those transfer function parameters that give the best agreement between the model output and the measured output. Third, validation tests assure that the resulting model accurately depicts the dynamic behavior of the process. Automation of this system identification procedure within a control system provides an on-line automatic tuning or adaptive mechanism that requires little or no operator intervention.

1.7. Input excitation

The classical excitation method is to subject the process to a step change in some manipulated variable and subsequently measure the open loop response of one or more measured variables. This step response method has been reportedly used for identification of extruder dynamics (Moreira et al., 1990; Lu et al., 1993; Cayot et al., 1995). However, such step response tests only excite low frequency components of the process. They often are unable to sufficiently excite the process at its −180° phase crossover frequency and result in dynamic models that do not reflect the process well at these higher frequencies. Incorrect modeling of dynamics at the phase crossover frequency can result in derived controller parameters that provide unstable closed-loop behavior (Åström & Hagglund, 1984). Thus, depending on the complexity of the process dynamics, a transfer function derived from step response tests may not be a good model for closed-loop control design.

Another common method used to excite the process dynamics is to modulate the manipulated variable according to an input profile based on a pseudo-random binary sequence (*PRBS*). Similar to the step response, this method is also performed in open loop. Such methods have also been applied to system identification of extruder dynamics (Hofer & Tan, 1993; Chang & Tan, 1993a, b). *PRBS* patterns are capable of exciting the process across a wide spectrum of frequencies. However, because *PRBS* experiments are performed in open-loop, it may be difficult to know a priori the frequency range or magnitude to use for generating the input.

In contrast to the step response and PRBS methods, which are performed in open loop, relay feedback is an alternative method for providing input excitation in closed loop. The fact that relay feedback is done in closed loop allows processes that are open loop unstable (e.g., integrated processes) to be stabilized during system identification experiments. For system identification, relay feedback has the important advantage that little or no a priori information about the dynamic behavior of the process is required. Under relay feedback, many processes exhibit limit cycle oscillations at their natural frequency. Once relay oscillations are initiated, the magnitude of the input signal can be adjusted in real time to achieve minimal output oscillation amplitude. This feature can be important, for example, if the identification is done during manufacturing where output variation must be kept to a minimum. Since relay feedback provides direct information regarding the natural frequency of the process, it has been used to derive automatic tuning parameters on-line for proportional-integral-derivative (PID) controllers (Åström, Hagglund & Wallenborg, 1993). More importantly, relay feedback has also been used as a method to provide input excitation for subsequent estimation of transfer function model parameters (Åström & Hagglund, 1984; Åström, 1988; Åström et al., 1993).

1.8. Transfer function modeling

Processes regulated by digital controllers are often modeled using a discrete time transfer function such as the following *z*-transform:

$$A(z^{-1})y(k) = \frac{B(z^{-1})}{F(z^{-1})}u(k) + \frac{C(z^{-1})}{D(z^{-1})}e(k). \quad (2)$$

Discrete time transforms have been described in the food engineering literature as a means to model the time dependent behavior of processes (Salvadori, Sanz, Alonso & Mascheroni, 1994). The z-transform exhibits a time shift property. That is, for example, $z^{-1}y(k) = y(k-1)$. This property makes the z-transform an extremely valuable tool for the study of discrete time systems. In Eq. (2), A, F, C and D are polynomials in z^{-1} that are monic (i.e., the leading polynomial coefficients, a_0, f_0, c_0 and d_0, equal 1), B is a polynomial in z^{-1} whose number of leading zero-valued coefficients equal the time delay in units of the sampling interval. The integer k denotes the discrete time sampling instant ($k = 0, 1, 2, \ldots$). The variables $u(k)$ and $y(k)$ denote the values of the process input and output, respectively at sampling instant k. Polynomials A, F and D describe the present output in terms of past values of the output. Discrete-time models that incorporate these polynomials are often referred to as having *auto-regressive* components. The polynomial B describes the present output in terms of present and past values of the input. Models that use these polynomials are often referred to as having external or *exogenous* components. The polynomial C describes the present output in terms of present and past values of process disturbances. Models with these polynomials are referred to as having *moving average* components.

While Eq. (2) represents an extremely flexible model structure, it is much too general to use in practical applications. Therefore, the model structure for a particular process of interest is made by combining only some auto-regressive components with possibly some moving average and exogenous components. Finding a suitable model structure thus involves determining the order of those polynomials in Eq. (2) that best mimic the dynamic behavior of the process. Using a set of process input and output data, any selected model structure can be parameterized. The final model structure selected to represent the process dynamics should be a trade-off between flexibility and accuracy. In most cases, this is the simplest model structure that best minimizes some residual error norm. Prior knowledge of time delays and disturbance characteristics can help to formulate an initial model structure that can then be verified through experimentation.

Different parameter estimation algorithms are available for model development. These algorithms differ by (1) which objective function is used to search for parameters, (2) which simplifying assumptions and approximations are made and (3) how process disturbances are handled. Different estimation methods have different convergence and parameter accuracy properties that depend on the number of measurement samples available, the statistical distribution of disturbance noise, the signal-to-noise ratio in the measurement data, the model structure selected and whether they are implemented as a recursive or as a batch algorithm. Consequently, the success or failure of any one method to converge to a set of satisfactory parameter estimates can depend on the initial parameter estimates used, the number of data samples evaluated, and whether any mechanisms are employed to restrain the estimated parameters to values that result in a stable transfer function estimate. In addition, parameter estimation algorithms can be further grouped according to whether they are implemented as a batch or recursive identification method. Batch identification is performed after the process data have been collected and stored, whereas recursive identification is performed every sampling instant as new process data become available. Batch identification methods analyze a segment of the input–output data together as a group, and therefore, are good candidates for time-invariant processes whose model parameters do not need to be frequently updated. Batch identification often requires a large amount of computational memory that is proportional to the number of data samples analyzed. In contrast, recursive identification methods provide updated parameter estimates at each sample interval as newly acquired input–output data become available. Recursive methods are good candidates for time-varying processes whose model parameters require frequent updating. The amount of memory required for recursive identification is proportional to the number of parameters to be estimated and is typically much smaller than that required for batch algorithms. Batch identification methods can accommodate complex non-linear optimization methods that require numerical analysis, whereas recursive methods can only provide an approximation to these methods. Consequently, for a given parameter estimation algorithm, the batch implementation may provide better parameter estimates than its corresponding recursive implementation. The bottom line is that if computer memory is available and if model parameters do not need to be updated at every sampling instant then batch estimation is probably the method of choice. Otherwise, recursive estimation should be considered.

1.9. Validation

Once a transfer function has been estimated, the resulting model is validated against an independent set of process input and output data that have not been used for model development or training. The performance of a model trained on one data set and evaluated using another independent data set is considered statistically significant for assessing confidence in the model (Ripley, 1996). Several objective measures to evaluate model performance are time and frequency domain error norms, the location and variance of estimated poles and zeros, residual error correlation and normality tests.

2. Experimental objectives

It is important to note that while system identification experiments for high shear twin-screw extrusion processes have been reported in the literature, no analysis has been presented that evaluates the use of relay feedback as an on-line system identification method. Furthermore, we could not find any research that compares the various parameter estimation methods and their batch and recursive implementations. Such information is required to develop automatic tuning and adaptive control systems for extrusion processing. Therefore, the specific experimental objectives of this work were to (1) evaluate relay feedback as an excitation method to identify the dynamic behavior of an extrusion cooking process and (2) evaluate various parameter estimation methods for deriving suitable transfer function models. Based on the system analysis presented earlier, the dynamic response of *ML* to changes in *SS* over a range of extrusion processing conditions was examined.

3. Materials and methods

All experimental studies were conducted using a co-rotating twin screw extruder with a screw diameter of 52 mm (Model TX-52 Wenger Manufacturing; Sabetha, KS) driven by a 22.37 kW (30 hp) DC drive motor. The extruder barrel was of a clamshell design, and was horizontally split and vertically segmented into modules or barrelheads. Each head had a length of five screw diameters that were internally cored to permit external heating or cooling of the extrudate using a suitable heat transfer fluid. All extruder variables could be visually monitored and manually adjusted at the operator's control panel.

During the experimental studies, all processing conditions were continuously measured by sensors located on the extruder. Five experimental runs were conducted, one under medium shear conditions and four under high shear conditions. In the medium shear experiment, the measurements were automatically recorded at a rate of 0.5 Hz by a Yokogawa 2400 digital data recorder. An IBM P-70 personal computer running Yokogawa HR 2400S data acquisition software was used to collect the data logged from the data recorder via an RS-232 serial protocol. The collected data was stored onto a diskette for later analysis.

In the high shear experiments, the measurements were automatically recorded at a rate of 10 Hz via an IBM ADC card that was interfaced directly to the backplane of an IBM XT personal computer. The software used to acquire and archive the measurement data was Asystant+(Version 1.0) supplied by McMillan and Company (1987). All analyses were performed using MATLAB version 4.2b and SIMULINK version 1.3a (The MathWorks; Natick, MA). The comparison of various parameter estimation methods was done using the MATLAB System Identification Toolbox, version 3.0a.

FR was controlled via the screw conveyor in the preconditioning cylinder. This conveyor transported the dry feed ingredients from a gravity-fed bin to the feed inlet of the extruder barrel. *SS* was regulated by a motor speed controller. The motor speed set-point was designated by an external low voltage signal provided through a potentiometer on the control panel. Using this potentiometer, *SS* could be manually adjusted to between 0 and 500 rpm ± 1 rpm. The rated screw speed was 355 rpm. *MC* was maintained by introducing ambient temperature water (*WA*) into the extruder barrel between heads 1 and 2 using a single speed variable stroke positive displacement pump. The flow rate of *WA* was visually monitored using flow meters and adjusted by setting the stroke of the water pump according to the following mass balance equation (Lu et al., 1992)

$$WA = FR\left(\frac{MC - FM}{1 - MC}\right). \tag{3}$$

TM was measured using a thermocouple that penetrated 0.5 inch into the flowing melt stream. The thermocouple was secured by a custom-made collar that was placed between the last barrelhead and the die.

4. Experimental procedures

The processing conditions and product formulation for the medium shear experiment are listed in Tables 1 and 2, respectively. This set of conditions and formulation was designed to give an unexpanded breakfast cereal product suitable for subsequent flaking or puffing with carbon dioxide gas. The screw configuration for the medium shear study was developed as part of ongoing supercritical fluid extrusion process research at Cornell University (Sokhey, Rizvi & Mulvaney, 1995). In the medium shear experimental study, chilled water at approximately 4°C was pumped through barrel heads 5–9. This helped to maintain *TM* below 100°C at the die thus preventing direct expansion of the extrudate.

The processing conditions and proximate composition of corn flour used for the high shear experiments are listed in Tables 3 and 4, respectively. This set of conditions was designed to provide high-shear cooking and puffing via moisture flash off for a corn-based snack food product. During the high shear experiments, the barrel temperature was left uncontrolled. The screw configuration was provided by the extruder manufacturer as one typical for high shear applications. The feed ingredient used was corn flour obtained from Lauhoff Grain Company (Danville, IL).

Table 1
Extrusion processing conditions used for the medium shear experimental study. All values are nominal

SS (RPM)	*FR* (kg/min)	*ML* (%)	Feed moisture (%WB)	*WA* (kg/min)	*MC* (%WB)	*SME* (kJ/kg)	*TM* (°C)
150	0.39	38	9.9	0.1	27.9	312	53

Table 2
Feedstock formulation used for the medium shear experimental study

Ingredient	Composition (% wet basis)
Pre-gelatinized corn flour	55.5
Sugar	10.8
Gluten	9.1
Fiber	8.8
Non-fat dry milk solids	8.1
Whey protein concentrate	3.9
Whey protein isolate	2.2
Salt	1.1
Glycerol monostearate	0.4

4.1. Relay-feedback

Before each experiment, the extruder was brought to a steady-state operating condition. The initial steady-state condition for the medium shear experiment is listed in Table 1. The initial steady-state conditions for each of the four high shear experiments are listed in Table 2. Once steady state was achieved, the system dynamics were excited using relay feedback according to the following procedure:

1. After steady state was achieved, the nominal values of *ML* and *SS* were recorded.
2. A positive step change in *SS* of approximately 50 rpm was applied.
3. In response to the positive step change in *SS*, the *ML* response was observed to immediately increase followed by a gradual decrease.
4. When the value of *ML* decreased to approximately its initial steady-state value, a negative step change in *SS* of approximately 50 rpm was applied.
5. In response to the negative step change in *SS*, the response in *ML* was observed to immediately decrease followed by a gradual increase.
6. When the value of *ML* increased to approximately its initial steady state value, a positive step change in *SS* of approximately 50 rpm was again made.
7. Steps 3–6 were repeated for approximately 10–20 min.

4.2. Transfer function model development

To determine dynamic response models in the form of *z*-transfer functions, the input–output data from each experiment was detrended and then segregated into a training and validation set of approximately equal lengths of time. To determine a suitable model order, a screening study first was made. In the screening study, the batch maximum likelihood method (MATLAB function armax.m) was used to parameterize first, second and third-order models using the training data from each experimental test. The structures for these transfer function models are shown in polynomial and pole–zero form in Table 5. The poles are the roots of the denominator polynomial whereas the zeros are the roots of the numerator polynomials. The polynomial form of the transfer function depicts the parameters as identified by the estimation method. The pole–zero form was examined to give added perspective to the time-response of the various modes of the system. Confidence in using higher order models was in part determined by examining the standard deviation of the pole–zero estimates. After parameterization, the models were subjected to *SS* data from the validation tests. The root mean squared (*RMS*) error between the model predicted *ML* and the actual *ML* was then calculated. The model structure selected from the screening study was the simplest one that provided relatively small *RMS* errors during validation.

Once a model order was selected from this initial screening study, the data from each experiment was fit

Table 3
Extrusion processing conditions and proximate composition of corn flour used in the high shear experimental studies. All values are nominal

SS (RPM)	*FR* (kg/min)	*ML* (%)	Feed moisture (%WB)	*WA* (kg/min)	*MC* (%WB)	*SME* (kJ/kg)	*TM* (°C)
300	1.1	45	10.0	0.038	13.0	318	190
350	1.1	40	10.0	0.038	13.0	330	192
300	1.1	45	10.0	0.061	14.8	312	178
350	1.1	40	10.0	0.061	14.8	324	181

Table 4
Proximate composition of corn flour used in the high shear experimental studies

Component	Proximate composition (% wet basis)
Carbohydrate	78.6
Moisture	12.0
Protein	6.0
Fat	2.2
Fiber	0.6
Ash	0.6

using parameter estimation algorithms other than the batch output error method. This was done to determine whether another parameter estimation method could be found that would provide a better model than that provided by the batch maximum likelihood algorithm used in the screening study. Both batch and recursive implementations were evaluated. Table 6 lists the parameter estimation methods that were compared. For the recursive implementations, a forgetting factor of 0.98 was used. The forgetting factor is typically used with recursive algorithms to reduce errors caused by biased initial parameter estimates. Validation was performed as in the screening study by subjecting each derived transfer function model to the SS input sequence from the validation data set and then comparing the model-predicted output with the actual process output for that same sequence. The results of the validation studies were used as a basis for objective evaluation and comparison of the various parameter estimation algorithms.

5. Results and analysis

5.1. Time domain analysis

After completing the experimental tests, the data collected from each experiment was analyzed to deter-

Table 5
Model structures evaluated in the screening study

Model order	Pole–zero form	Polynomial form
1	$ML(k) = K\frac{z-\beta_1}{z-\alpha_1}SS(k) + \frac{z-\gamma_1}{z-\alpha_1}e(k)$	$ML(k) = \frac{b_0 + b_1 z^{-1}}{1 + a_1 z^{-1}}SS(k) + \frac{1 + c_1 z^{-1}}{1 + a_1 z^{-1}}e(k)$
2	$ML(k) = K\frac{z-\beta_1}{z-\alpha_1}\frac{z-\beta_2}{z-\alpha_2}SS(k) + \frac{z-\gamma_1}{z-\alpha_1}\frac{z-\gamma_2}{z-\alpha_2}e(k)$	$ML(k) = \frac{b_0 + b_1 z^{-1} + b_2 z^{-1}}{1 + a_1 z^{-1} + a_2 z^{-1}}SS(k) + \frac{1 + c_1 z^{-1} + c_2 z^{-1}}{1 + a_1 z^{-1} + a_2 z^{-1}}e(k)$
3	$ML(k) = K\frac{z-\beta_1}{z-\alpha_1}\frac{z-\beta_2}{z-\alpha_2}\frac{z-\beta_3}{z-\alpha_3}SS(k) + \frac{z-\gamma_1}{z-\alpha_1}\frac{z-\gamma_2}{z-\alpha_2}\frac{z-\gamma_3}{z-\alpha_3}e(k)$	$ML(k) = \frac{b_0 + b_1 z^{-1} + b_2 z^{-1} + b_3 z^{-1}}{1 + a_1 z^{-1} + a_2 z^{-1} + a_3 z^{-1}SS(k)} + \frac{1 + c_1 z^{-1} + c_2 z^{-1} + c_3 z^{-1}}{1 + a_1 z^{-1} + a_2 z^{-1} + a_3 z^{-1}}e(k)$

Table 6
List of parameter estimation methods compared

	Parameter estimation algorithm	Polynomials parameterized from Eq. (3)	MATLAB function
Batch	Least-squares	*A*, *B*	arx.m
	Output error	*B*, *F*	oe.m
	Prediction error	*B*, *C*, *D*, *F*	pem.m
	Maximum likelihood	*A*, *B*, *C*	armax.m
	Box–Jenkins	*B*, *C*, *D*, *F*	bj.m
Recursive	Least-squares	*A*, *B*	arx.m
	Extended least-squares	*A*, *B*, *C*	rplr.m
	Output error	*B*, *F*	roe.m
	Prediction error	*B*, *C*, *D*, *F*	rpem.m
	Maximum likelihood	*A*, *B*, *C*	rarmax.m
	Box–Jenkins	*B*, *C*, *D*, *F*	rbj.m

mine a suitable discrete-time transfer function that would adequately depict the dynamic response of *ML* to changes in *SS*. The *SS* and corresponding *ML* response for each of the five experimental tests are plotted in Figs. 2–6. In each of these experimental test results, it is noted that the *ML* response to step change in *SS* is typical of lead-lag type dynamics. This response is characterized by an immediate overshoot followed by an inverse response. The new steady state achieved by *ML* was observed to be either slightly greater than, close to or less than its original nominal value. This lead-lag dynamic response is what is to be modeled using on-line system identification.

The dynamic response found in this study can be compared with those presented by Lu et al. (1993). Using off-line techniques, they determined the dynamic response of torque to step changes in *SS* during high shear extrusion processing of a cooked, directly expanded corn meal product using an APV-Baker 50 mm twin screw extruder. They also found an inverse response of torque to changes in *SS*. The similarity in the dynamic response as presented by Lu et al. (1993) with the results found in this study confirms that an inverse response model can be used, but that the model parameters may vary depending on the operating and processing conditions.

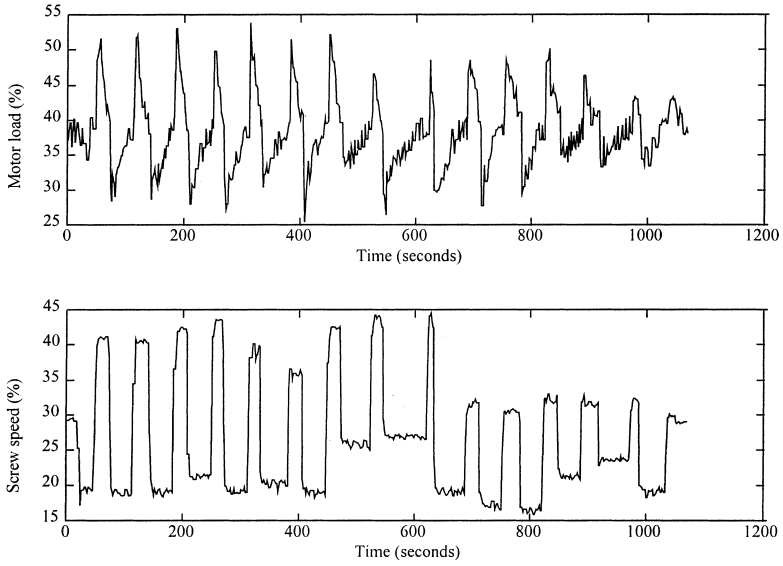

Fig. 2. Experimental results of *SS* and *ML* under medium shear operating conditions. $SS = 150\,RPM$, $MC = 27.9\%$.

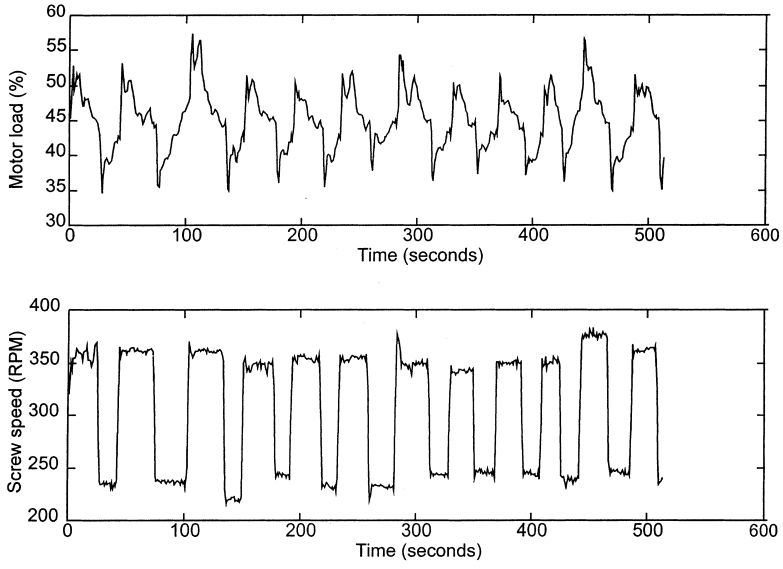

Fig. 3. Experimental results of *SS* and *ML* under high shear operating conditions. $SS = 300\,RPM$, $MC = 13.0\%$.

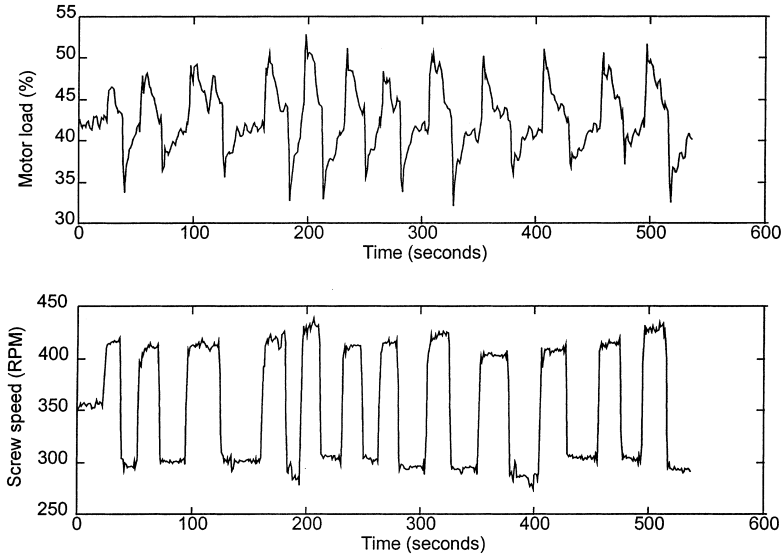

Fig. 4. Experimental results of *SS* and *ML* under high shear operating conditions. $SS = 350\,RPM$, $MC = 13.0\%$.

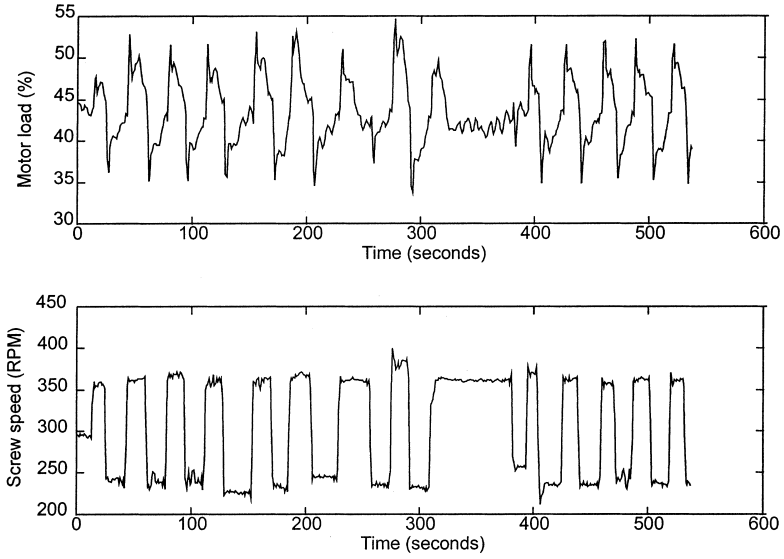

Fig. 5. Experimental results of *SS* and *ML* under high shear operating conditions. $SS = 300\,RPM$, $MC = 14.8\%$.

5.2. Frequency domain analysis

An *estimated* frequency response analysis of *ML* and *SS* was made using the Matlab supplied spectral analysis function contained in the script file 'spa.m'. Fig. 7 shows the estimated magnitude and Fig. 8 shows the estimated phase for the five experimental studies. The results indicate that the magnitude of the frequency response in the medium shear experiment appeared more uniformly distributed across frequencies than in the high shear experiments. The high shear experiments show significantly more high frequency content than the medium shear experiment. This effect may be due to the difference in feedstock composition between the high shear and medium shear studies. It may also be due to the higher screw speed used in the high shear experiments. The effect of *MC* on the phase lag is clearly demonstrated in the high shear experimental studies. Fig. 8 indicates that above 0.6 rad/sec, those experimental studies with $MC = 13.0\%$ exhibited a greater phase-lag than those experimental studies with $MC = 14.8\%$. Thus, it appears that feed formulation, particularly *MC*, affected the dynamic response of the extruder more strongly than did *SS* at these frequencies. This is consistent with the view expressed earlier that moisture content really defines the 'polymer' being ex-

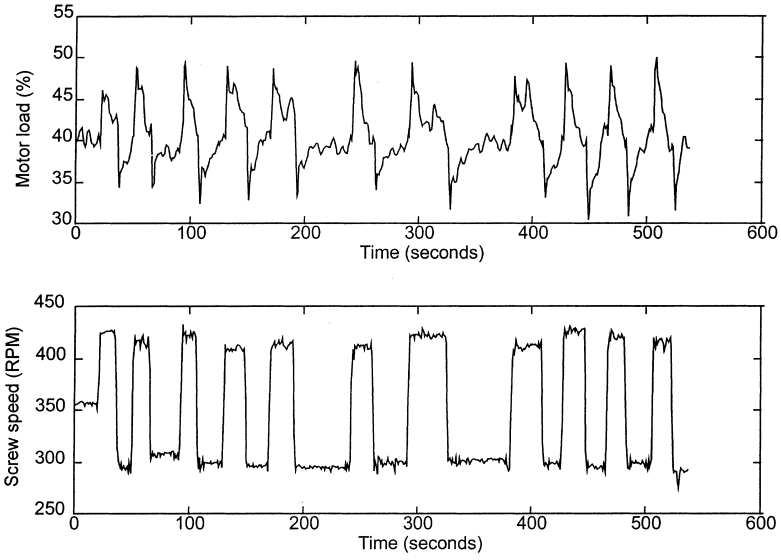

Fig. 6. Experimental results of *SS* and *ML* under high shear operating conditions. $SS = 350\,RPM$, $MC = 14.8\%$.

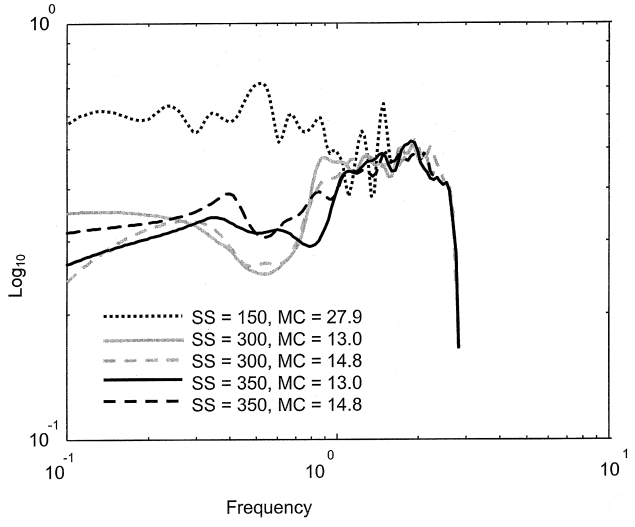

Fig. 7. Results of estimated magnitude versus frequency for the five experimental studies.

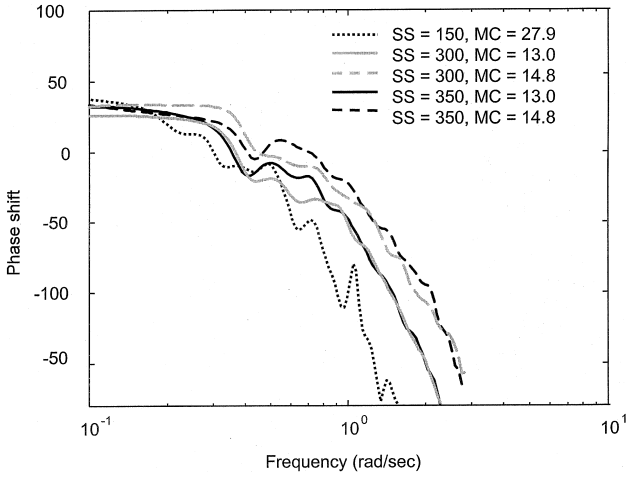

Fig. 8. Results of estimated phase shift versus frequency for the five experimental studies.

truded. Accurate modeling at frequencies close to the −180° phase crossover frequency is important for systems controlled by negative unity feedback. The magnitude of the system at this frequency must be well below unity for closed-loop stability and robustness. This result indicates that a closed-loop controller tuned for 30° phase margin under conditions where the *MC* is 14.8% may exhibit instability if the *MC* drops to 13% or lower. Consequently, it may be more important to identify a new transfer function when changes or disturbances in feed formulation occur than when a change in *SS* occurs. This is especially important since a common disturbance in extrusion processing is variation in *MC* due to differences in the feed moisture content.

5.3. Model structure parameterization

Tables 7–11 list the gain, zero and pole values, their standard deviations and the root mean square (*RMS*) error as estimated by the batch maximum likelihood method during the initial screening study. It was noted that each discrete-time transfer function was found to have a zero whose value was close to 1.0 in the *z*-plane. This zero reflects the lead dynamics of *ML* in response to changes in *SS*. Furthermore, it was found that each transfer function had a dominant pole located between 0.75 and 0.93 in the *z*-plane. This pole reflects the lag dynamics of *ML* in response to changes in *SS*. This zero–pole pair is consistent with the lead-lag dynamic response observed. It was observed that the poles estimated in the second and third-order models represented

Table 7
Results of model structure screening study. $SS = 150$ *RPM*, $MC = 27.90\%$

Model order	Steady state gain (s.d.)	Zeros			Poles			*RMS* error
		β_1 (s.d.)	β_2 (s.d.)	β_3 (s.d.)	α_1 (s.d.)	α_2 (s.d.)	α_3 (s.d.)	
1	−0.2896 (0.1244)	1.0325 (0.0205)			0.9373 (0.0195)			2.4174
2	−0.6846 (0.2690)	1.0486 (0.0191)	0.6899 (0.1773)		0.9655 (0.0188)	0.6202 (0.1930)		2.3247
3	−0.6824 (0.2778)	1.0510 (0.0202)	0.5988 (0.2315) 0.0349i (0.0637i)	0.5988 (0.2582) −0.0349i (0.0637i)	0.9642 (0.0195)	0.6889 (0.3483)	0.3515 (0.3312)	2.3190

Table 8
Results of model structure screening study. $SS = 300$ *RPM*, $MC = 13.0\%$

Model order	Steady state gain (s.d.)	Zeros			Poles			*RMS* error
		β_1 (s.d.)	β_2 (s.d.)	β_3 (s.d.)	α_1 (s.d.)	α_2 (s.d.)	α_3 (s.d.)	
1	0.0267 (0.0963)	0.9922 (0.0298)	–	–	0.8977 (0.0278)	–		1.5929
2	0.0786 (0.0490)	0.9722 (0.0201)	−0.8114 (0.1209)	–	0.8397 (0.0256)	−0.3373 (0.0870)		1.6164
3	−0.0549 (0.1055)	1.0148 (0.0255)	−0.9347 (0.0845)	0.2171 (0.1234)	0.9049 (0.0268)	−0.0975 (0.0482) 0.3902i (0.0777i)	0.0975 (0.5014) −0.3902i (0.0777i)	1.5351

Table 9
Results of model structure screening study. $SS = 350$ *RPM*, $MC = 13.0\%$

Model order	Steady state gain (s.d.)	Zeros			Poles			*RMS* error
		β_1 (s.d.)	β_2 (s.d.)	β_3 (s.d.)	α_1 (s.d.)	α_2 (s.d.)	α_3 (s.d.)	
1	0.0874 (0.0599)	0.9673 (0.0276)	–	–	0.8612 (0.0301)	–	–	1.1603
2	0.1367 (0.0332)	0.9384 (0.0202)	−1.4539 (0.1006)	–	0.7974 (0.0263)	−0.6161 (0.0466)	–	1.1558
3	0.0611 (0.0689)	0.9805 (0.0260)	−1.5083 (0.0819)	0.2980 (0.1569)	0.8808 (0.0337)	−0.6206 (0.0522)	0.1677 (0.1635)	1.0649

fast dynamics that are not of interest from a control design perspective. In addition, since the standard deviations of the higher order poles and zero estimates were larger than those for the first-order models, less confidence could be placed in them.

Next, a validation study of each model was made by subjecting each of the first-, second- and third-order transfer functions to the *SS* data from the validation data sets. The output predicted by each model was then compared to the corresponding *ML* output from the validation sets. A comparison of the *infinite-step-ahead* model prediction with the actual *ML* response for the medium shear experimental study ($SS = 150$ rpm and $MC = 27.9\%$) is shown in Fig. 9. This figure illustrates that the first-order model adequately captured the dominant process dynamics and that a second-order model contributed little to improving the fit to the experimental data. An analysis of the residual errors obtained during the validation study was made using auto correlation, cross correlation and normality tests. The results from these analyses provided further evidence that little if any information remained in the error re-

Table 10
Results of model structure screening study. $SS = 300$ *RPM*, $MC = 14.8\%$

Model order	Steady state gain (s.d.)	Zeros			Poles			*RMS* error
		β_1 (s.d.)	β_2 (s.d.)	β_3 (s.d.)	α_1 (s.d.)	α_2 (s.d.)	α_3 (s.d.)	
1	0.0898 (0.0302)	0.9479 (0.0210)	–	–	0.7594 (0.0253)	–	–	2.0469
2	−0.0813 (0.1275)	1.0249 (0.0312)	0.4805 (0.1107)	–	0.9154 (0.0348)	0.2317 (0.1063)	–	1.7845
3	−0.0239 (0.0520)	1.0092 (0.0186)	0.7842 (0.0319) 0.3644i (0.0368i)	0.7842 (0.0618) −0.3644i (0.0368i)	0.7875 (0.1134)	0.7130 (0.0721) 0.2217i (0.0903i)	0.7130 (0.5159) −0.2217i (0.0903i)	1.6698

Table 11
Results of model structure screening study. $SS = 350$ *RPM*, $MC = 14.8\%$

Model order	Steady state gain (s.d.)	Zeros			Poles			*RMS* error
		β_1 (s.d.)	β_2 (s.d.)	β_3 (s.d.)	α_1 (s.d.)	α_2 (s.d.)	α_3 (s.d.)	
1	0.1083 (0.0275)	0.9349 (0.0208)	–	–	0.7495 (0.0264)	–	–	1.5148
2	0.0518 (0.0587)	0.9769 (0.0313)	0.4607 (0.2212)	–	0.8582 (0.0528)	0.3045 (0.2009)	–	1.4313
3	0.1084 (0.0322)	0.9305 (0.0265)	0.5108 (0.0284) 0.7211i (0.0323i)	0.5108 (0.0748) −0.7211i (0.0323i)	0.7552 (0.0339)	0.4642 (0.0298) 0.7235i (0.0297i)	0.4642 (0.0666) −0.7235i (0.0297i)	1.5832

siduals from a first-order model fit to justify using a higher order model. The details of the residual error analyses conducted during the screening study can be found in Haley (1998). The results of the screening study suggested that a first-order model structure would adequately depict the dominant behavior of the *SS* to *ML* dynamics such that

$$ML(k) = G(z)SS(k), \tag{4}$$

where

$$G(z) = \frac{b_0 + b_1 z^{-1}}{1 + a_1 z^{-1}}.$$

It was apparent that the higher order transfer functions were simply modeling some of the high frequency disturbances that reside outside the frequency bandwidth of interest for process control design.

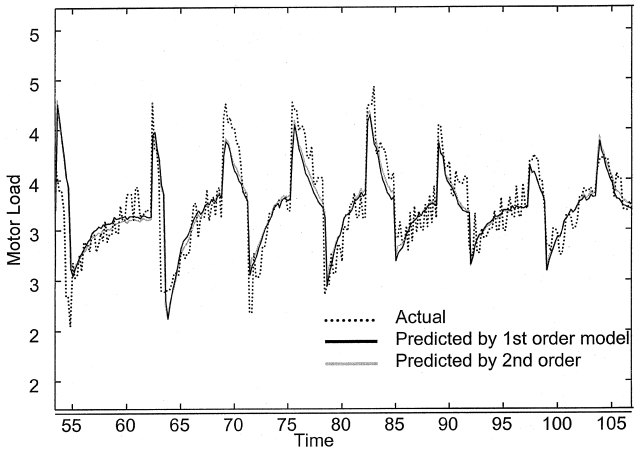

Fig. 9. Comparison of actual versus model predicted output using 1st and 2nd order models as estimated by the batch maximum likelihood method. Medium shear experimental study. $SS = 150$, $MC = 27.9\%$.

5.4. Evaluation of parameter estimation methods

Tables 11–16 detail the gain, zero and pole values, their standard deviations and the root mean square (*RMS*) error found for each model generated by the various parameter estimation methods for each of the five experimental studies. It is noteworthy that no *one* parameter estimation method clearly stands out among others as superior in terms of providing a significantly smaller *RMS* error. However, it can be seen that the recursive prediction error method (rpem.m) and the

Table 12
Estimated parameters, their mean and standard deviation, and RMS error of transfer function models identified by different estimation algorithms $SS = 150$ RPM, $MC = 27.9\%$

Implementation	Parameter estimation algorithm	Gain (s.d.)	Zero (s.d.)	Pole (s.d.)	*RMS* error
Batch	Least-squares	0.0121	0.9973	0.8734	2.9076
		(0.0867)	(0.0365)	(0.0343)	
	Output error	−0.3028	1.0295	0.9430	2.3999
		(0.0712)	(0.0101)	(0.0109)	
	Prediction error	−0.3376	1.0321	0.9466	2.3792
		(0.1056)	(0.0142)	(0.0145)	
	Maximum likelihood	−0.2896	1.0325	0.9373	2.4174
		(0.1244)	(0.0205)	(0.0195)	
	Box–Jenkins	−0.3367	1.0321	0.9465	2.3797
		(0.1057)	(0.0143)	(0.0145)	
Recursive	Extended least-squares	−0.3076	1.0394	0.9338	2.4565
		(0.3064)	(0.0542)	(0.0472)	
	Least-squares	0.0207	0.9948	0.8794	3.0150
		(0.1101)	(0.0527)	(0.0439)	
	Output error	−0.2553	1.0263	0.9425	2.4385
		(0.0787)	(0.0123)	(0.0128)	
	Prediction error	0.0237	0.9937	0.8687	3.0377
		(0.2620)	(0.1356)	(0.1408)	
	Maximum likelihood	−0.2668	1.0363	0.9323	2.5049
		(0.2464)	(0.0476)	(0.0419)	
	Box–Jenkins	0.0237	0.9937	0.8687	3.0377
		(0.2620)	(0.1356)	(0.1408)	

Table 13
Estimated parameters, their mean and standard deviation, and RMS error of transfer function models identified by different estimation algorithms. $SS = 300$ RPM, $MC = 13.0\%$

Implementation	Parameter estimation algorithm	Gain (s.d.)	Zero (s.d.)	Pole (s.d.)	*RMS* error
Batch	Least-squares	0.0027	0.9993	0.9042	1.5163
		(0.0802)	(0.0208)	(0.0203)	
	Output error	−0.2361	1.039	0.9419	1.4551
		(0.0617)	(0.007)	(0.0069)	
	Prediction error	−0.3995	1.054	0.9571	1.4887
		(0.1339)	(0.0102)	(0.0087)	
	Maximum likelihood	0.0267	0.9922	0.8977	1.5929
		(0.0963)	(0.0298)	(0.0278)	
	Box–Jenkins	−0.3934	1.0533	0.9567	1.4848
		(0.1338)	(0.0102)	(0.0089)	
Recursive	Extended least-squares	0.1114	0.9591	0.8592	1.6813
		(0.1301)	(0.061)	(0.0682)	
	Least-squares	0.0152	0.9959	0.9039	1.5578
		(0.2191)	(0.0614)	(0.0595)	
	Output error	0.0479	0.986	0.8937	1.5844
		(0.0482)	(0.0157)	(0.0195)	
	Prediction error	−0.2061	1.0376	0.9367	1.4620
		(0.1246)	(0.0173)	(0.0149)	
	Maximum likelihood	0.1784	0.9113	0.8212	1.9473
		(0.1329)	(0.0929)	(0.0946)	
	Box–Jenkins	−0.2061	1.0376	0.9367	1.4620
		(0.1246)	(0.0173)	(0.0149)	

recursive Box–Jenkins method (rbj.m) performed significantly more poorly than the other parameter estimation algorithms in the experimental studies where $MC = 14.8\%$. These algorithms have special data requirements for accurate parameter convergence (Ljung & Soderstrom, 1983) that may not have been met by these particular experimental data sets. These results also reflect the observations made by Johnson (1988)

Table 14
Estimated parameters, their mean and standard deviation, and RMS error of transfer function models identified by different estimation algorithms. $SS = 300$ RPM, $MC = 13.0\%$

Implementation	Parameter estimation algorithm	Gain (s.d.)	Zero (s.d.)	Pole (s.d.)	*RMS* error
Batch	Least-squares	0.0402	0.9811	0.8193	1.8990
		(0.0348)	(0.0177)	(0.0208)	
	Output error	−0.0628	1.0177	0.9022	1.8477
		(0.0327)	(0.008)	(0.0102)	
	Prediction error	0.0356	0.9857	0.8364	1.9012
		(0.0359)	(0.0156)	(0.0208)	
	Maximum likelihood	0.0898	0.9479	0.7594	2.0469
		(0.0302)	(0.021)	(0.0253)	
	Box–Jenkins	0.0427	0.9822	0.8298	1.9116
		(0.0354)	(0.0163)	(0.0219)	
Recursive	Extended least-squares	0.0335	0.9818	0.8063	1.9394
		(0.0771)	(0.0446)	(0.0551)	
	Least-squares	−0.0046	1.0022	0.8271	1.8539
		(0.0933)	(0.0439)	(0.0547)	
	Output error	−0.0253	1.0123	0.8453	1.8794
		(0.0266)	(0.0126)	(0.0162)	
	Prediction error	0.1476	0.788	0.4134	2.5293
		(0.1126)	(0.2221)	(0.2548)	
	Maximum likelihood	0.0566	0.9659	0.7513	2.0180
		(0.1087)	(0.0722)	(0.0983)	
	Box–Jenkins	0.1476	0.788	0.4134	2.5293
		(0.1126)	(0.2221)	(0.2548)	

Table 15
Estimated parameters, their mean and standard deviation, and RMS error of transfer function models identified by different estimation algorithms. $SS = 350$ RPM, $MC = 13.0\%$

Implementation	Parameter estimation algorithm	Gain (s.d.)	Zero (s.d.)	Pole (s.d.)	*RMS* error
Batch	Least-squares	0.1101	0.9619	0.8679	1.1296
		(0.0500)	(0.0221)	(0.0237)	
	Output error	0.0680	0.9800	0.8798	1.0823
		(0.0217)	(0.0077)	(0.0114)	
	Prediction error	0.0301	0.9921	0.8991	1.0739
		(0.0499)	(0.0142)	(0.0185)	
	Maximum likelihood	0.0874	0.9673	0.8612	1.1603
		(0.0599)	(0.0276)	(0.0301)	
	Box–Jenkins	0.0387	0.9897	0.8954	1.0774
		(0.0412)	(0.0121)	(0.0162)	
Recursive	Extended least-squares	0.0896	0.9696	0.8700	1.1053
		(0.1876)	(0.0772)	(0.0783)	
	Least-squares	0.0916	0.9688	0.8691	1.1068
		(0.1563)	(0.0645)	(0.0640)	
	Output error	−0.1550	1.0272	0.9334	1.2517
		(0.1938)	(0.0255)	(0.0251)	
	Prediction error	−0.0552	1.0112	0.9188	1.1883
		(0.3436)	(0.0624)	(0.0659)	
	Maximum likelihood	0.1306	0.9502	0.8533	1.1705
		(0.1726)	(0.0876)	(0.0891)	
	Box–Jenkins	−0.0552	1.0112	0.9188	1.1883
		(0.3436)	(0.0624)	(0.0659)	

that the capacity for a signal to provide persistent excitation depends partly on the parameter estimation algorithm used.

Of the algorithms evaluated, the batch output error algorithm appeared to provide consistently good results, in terms of small parameter standard deviations and

Table 16
Estimated parameters, their mean and standard deviation, and RMS error of transfer function models identified by different estimation algorithms. $SS = 350$ *RPM*, $MC = 14.8\%$

Implementation	Parameter estimation algorithm	Gain (s.d.)	Zero (s.d.)	Pole (s.d.)	*RMS* error
Batch	Least-squares	0.0796 (0.0254)	0.9607 (0.015)	0.7999 (0.0197)	1.4173
	Output error	0.1085 (0.0121)	0.9492 (0.0079)	0.7976 (0.0161)	1.4532
	Prediction error	0.1014 (0.0257)	0.9435 (0.0187)	0.7697 (0.0283)	1.4776
	Maximum likelihood	0.1083 (0.0275)	0.9349 (0.0208)	0.7495 (0.0264)	1.5148
	Box–Jenkins	0.1018 (0.0257)	0.9433 (0.0187)	0.7693 (0.0284)	1.4774
Recursive	Extended least-squares	0.0539 (0.1)	0.9745 (0.0527)	0.8261 (0.0619)	1.4278
	Least-squares	0.026 (0.1238)	0.9896 (0.0521)	0.851 (0.0608)	1.3753
	Output error	0.0718 (0.0352)	0.9709 (0.0174)	0.8219 (0.0327)	1.3861
	Prediction error	−0.6412 (0.1019)	−14.8158 (22.7065)	0.2822 (0.0621)	9.5226
	Maximum likelihood	0.0555 (0.1343)	0.9723 (0.0747)	0.8143 (0.0855)	1.4360
	Box–Jenkins	−0.6412 (0.1019)	−14.8158 (22.7065)	0.2822 (0.0621)	9.5226

small *RMS* error residuals, across the range of product and processing conditions studied. A good fit by the output error method indicates that, within the frequency bandwidth of interest, disturbances noted in the output measurements are not coupled with the process inputs. Using the validation data set from the medium shear experimental study as an example, a comparison between the batch output error model and actual system response is plotted in Fig. 10 (cf. Fig. 9). Fig. 11 shows the corresponding auto and cross correlation plots of the residual errors, and Fig. 12 shows a histogram of the residual error versus frequency of occurrence. The auto and cross correlation tests show that the residual errors correlate no better than that expected for white noise. The histogram shows that the residual errors closely approximate a Gaussian distribution. These results indicate that the batch output error parameter estimation method could derive a first-order transfer function parameterization that adequately describes the dynamic response of *ML* to changes in *SS*. Furthermore, the

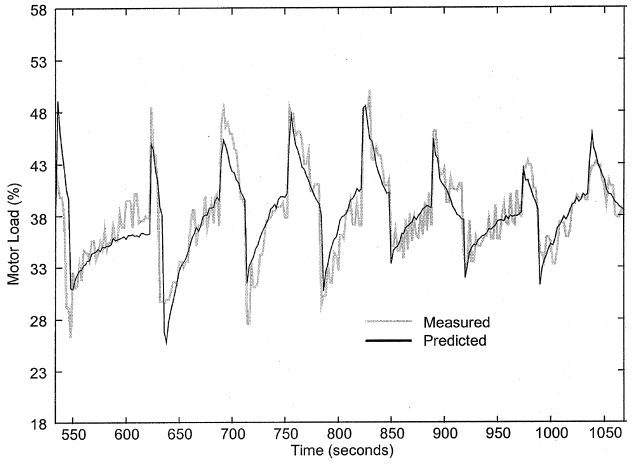

Fig. 10. Comparison of actual versus model predicted output using 1st order model as estimated by the batch output error method. Medium shear experimental study, $SS = 150$, $MC = 27.9\%$.

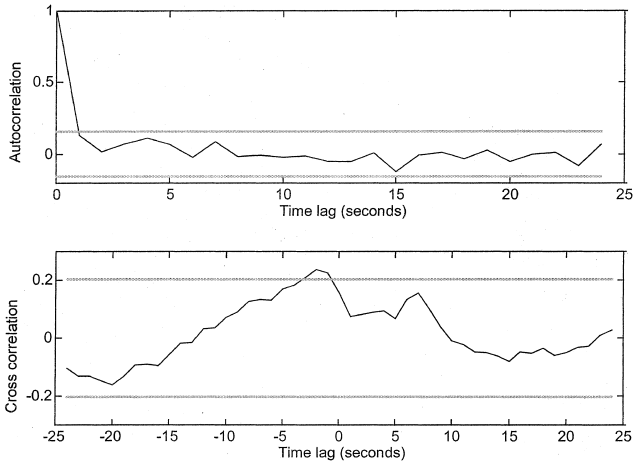

Fig. 11. Auto and cross correlation of residual errors using 1st order model as estimated by the batch output error method. Medium shear experimental study. $SS = 150$ *RPM*, $MC = 27.9\%$.

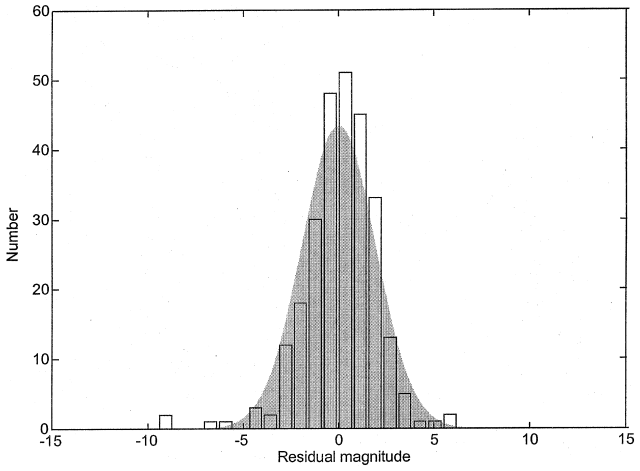

Fig. 12. Histogram showing the residual error magnitude versus frequency using a 1st order model as estimated by the batch output error method. Medium shear experimental study. $SS = 150\,RPM$, $MC = 27.9\%$.

residual error that resulted from using the estimated transfer function contained no additional information to justify the use of a more complex transfer function structure. Similar results were found for the high shear experimental studies.

As a final observation, it is interesting to note that the model parameters appeared particularly sensitive to *MC*. For the high shear experiments where the feedstock was composed entirely of corn flour and water, the lag dynamics (pole locations) of *ML* to changes in *SS* were found to correlate with *MC*. Specifically, it was noted that the speed of the response had a positive correlation with the *MC*. However, it was observed that the speed of response of *ML* was considerably slower in the medium shear experiment compared to that in the high shear experiments even though the *MC* was considerably higher (27.9%). Since the formulation, screw speed and screw configuration were significantly different in the medium shear versus high shear experiments, it is evident that these factors have a significant impact on process dynamics. This observation further supports the view that some means of on-line system identification for automatic tuning application in extrusion cooking control systems is warranted. In fact, these observations may explain why extruder vendors do not provide 'turn-key' closed loop control systems with their extruders.

6. Conclusion

This paper has described the development and comparative evaluation of on-line system identification methods for a twin-screw extrusion cooking process. We found relay-feedback to be a good excitation method for inclusion as a method for excitation in an on-line system identification system. We also found the batch output error parameter estimation algorithm to provide good transfer function model parameters across a wide range of product and processing conditions. The system identification procedure described in this paper can be used as part of an automatic tuning and adaptive control system. The demonstration of such a system for control of extrudate density is the topic of the subsequent paper in this two part series.

References

Åström, K. J. (1988). Method and an apparatus for automatically tuning a process regulator. *Hightech Network AB*, Malmo, Sweden:US, 1–10.

Åström, K. J., Hagglund, T. (1984). Automatic tuning of simple regulators with specifications on phase and amplitude margins. *Automatica*, *20*, 645.

Åström, K. J., Hagglund, T., & Wallenborg, A. (1993). Automatic tuning of digital controllers with applications to HVAC plants. *Automatica 29*, 1333.

Cayot, N., Bounie, D., & Baussart, H. (1995). Dynamic modelling for a twin screw food extruder: analysis of the dynamic behaviour through process variables. *Journal of Food Engineering*, 245–259.

Chang, Z., & Tan, J. (1993a). Determination of model structure for twin-screw food extrusion – Part 1 Multi-loop. *TransIChemE*, *71*, 11–19.

Chang, Z., & Tan, J. (1993b). Determination of model structure for twin-screw food extrusion – Part 2 Multi-variable. *TransIChemE*, *71*, 20–26.

Haley, T. A. (1998). On-line system identification and control design for extrusion cooking and puffing processes. Ph.D. Dissertation, Cornell University.

Hofer, J., & Tan, J. (1993). Extrudate temperature control with disturbance prediction. *Food Control*, *4*, 17–24.

Johnson, C. R., Jr. (1988). *Lectures on adaptive parameter estimation.* Englewood Cliffs: Prentice-Hall.

Kulshreshtha, M. K., Zaror, C. A., Jukes, D. J. (1991). Automatic control of food extrusion problems and perspectives. *Food Control*, 80–86.

Kulshreshtha, M. K., Zaror, C. A., & Jukes, D. J. (1995). Simulating the performance of a control systems for food extruders using model based set point adjustment. *Food Control*, *6*, 135–141.

Kulshreshtha, M. K., Zaror, C. A., Jukes, D. J., Pyle, D. L. (1991). A generalized steady-state model for twin screw extruders. *Trans IChemE*, *69*, *Part c*, 189–199.

Ljung, L., Soderstrom, T. (1983). *Theory and practice of recursive identification.* Cambridge Massachusetts: MIT Press.

Lu, Q., Hsieh, F., Mulvaney, S. J., Tan, J., & Huff, H. E. (1992). Dynamic analysis of process variables for a twin-screw food extruder. *Food Control*, *4*, 261–270.

Lu, Q., Mulvaney, S. J., Hsieh, F., & Huff, H. E. (1993). Model and strategies for computer control of a twin-extruder. *Food Control*, *4*, 25–33.

Meuser, F., van Lengerich, B., & Kohler, F. (1982). Einfluss der extrusionparameter auf funktionelle eighenschaft von weizenstaerke. *Staerke*, *34*, 366.

Mohamed, I. O., Ofoli, R. Y. (1990). Prediction of temperature profiles in twin screw extruders. *Journal of food engineering*, 145–164.

Moreira, R. G., Srivastava, A. K., & Gerrish, J. B. (1990). Feedforward control model for a twin-screw food extruder. *Food Control*, *1*, 179–184.

Onwulata, C. I., Mulvaney, S. J., & Hsieh, F. (1994). System analysis as the basis for control of density of extruded cornmeal. *Food Control*, *5*, 39–48.

Ripley, B. D. (1996) *Pattern recognition and neural networks*. New York: Cambridge University Press.

Salvadori, V. O., Sanz, P. D., Alonso, D. M., & Mascheroni, R. H. (1994). Application of *z*-transfer functions to heat or mass transfer problems: their calculation by numerical methods. *Journal of Food Engineering*, *23*, 293–307.

Sokhey, A. S., Rizvi, S. S. H., & Mulvaney, S. J. (1995). Application of supercritical fluid extrusion to cereal processing. *Cereal Foods World*, *41*, 29–34.

Tayeb, J., Vergnes, B., & Valle, G. A (1989). Della basic model for a twin screw extruder. *Journal of Food Science*, *47*, 1047–1056.

Van Lengerich, B. (1990). Influence of extrusion processing on in-line rheological behavior, structure, and function of wheat starch. In H. Faridi & J. M. Faubion (Eds.), *Dough rheology and baked product texture* (p. 421). New York: AVI Van Nostrand Reinhold.

van Zuilichm, D., van der Laan, E., & Kuiper, E. (1990). The development of a heat transfer model for twin screw extruders. *Journal of Food Engineering*, 187–207.